IEEE Access
Multidisciplinary ⋮ Rapid Review ⋮ Open Access Journal

Received October 27, 2020, accepted November 7, 2020, date of publication November 10, 2020, date of current version December 1, 2020.

Digital Object Identifier 10.1109/ACCESS.2020.3037240

Analyses on Volatility Clustering in Financial Time-Series Using Clustering Indices, Asymmetry, and Visibility Graph

KYUNGWON KIM[1] **AND JAE WOOK SONG**[2]
[1]AI Center, Samsung Research, Samsung Electronics Seoul Research and Development Campus, Seoul 06765, South Korea
[2]Department of Industrial Engineering, Hanyang University, Seoul 04763, South Korea

Corresponding author: Jae Wook Song (jwsong@hanyang.ac.kr)

This work was supported by the research fund of Hanyang University under Grant HY-2019.

ABSTRACT The volatility clustering has critical implications in financial risk management. This paper aims to analyze the existence and cause of volatility clustering in financial time-series using different measures simultaneously. Specifically, we utilize the clustering indices, asymmetry measures, and the power of the scale freeness in the visibility graph. For the experiment, we utilize four representing financial time-series, including the S&P500, one-year US Treasury Constant Maturity rate, Euro-Dollar exchange rate, and Crude oil for the stock, bond, exchange, and commodity markets, respectively. The duration of the experiment is from 2009 to 2018, which is divided into two sub-periods: crisis and post-crisis periods. At first, we identify the positive and slowly decaying non-linear autocorrelation in all markets, which indicates the power-law decay. Also, the autocorrelation of the simulated time-series suggests that the order of return-series with respect to its magnitude contributes more to the volatility clustering than the heavy-tailed distributions. Secondly, we detect that the scale of the return contributes more to volatility clustering than the sign of the return. Lastly, we observe that the clustering and asymmetry measures are more robust measures to the return distribution changes than the PSVG to analyze the volatility clustering.

INDEX TERMS Clustering asymmetry, clustering index, finance, pattern clustering, power-law decay, statistical analysis, time series analysis, visibility graph, volatility clustering.

I. INTRODUCTION

The financial time-series and its associated return distribution, representing the market's volatility, are of great interest to both researchers and investors. In general, the financial time series are assumed to be independent and identically distributed (iid) generated from random walks [1]. Therefore, the probability density function of the return should follow the Gaussian distribution. However, the clustering of the large fluctuations in financial price-series is observed accompanying the return distribution's heavy tail property [2], [3]. In other words, a large fluctuation is likely to follow a previous large fluctuation, whereas a small fluctuation is likely to follow a previous small fluctuation, which rejects the iid assumption. Such a phenomenon is called the volatility clustering. The financial market is characterized by unexpected shocks. In this milieu, the volatility clustering has critical implications in financial risk management, especially in calculating the Value-at-Risk or Expected Shortfall of the portfolio. When an unexpected shock is realized, the volatility of a financial market dramatically increases. Furthermore, the existence of volatility clustering suggests the persistence of extreme volatility for a while. Given that the risk measures are estimated based on the historical return series, investors must adjust the estimates to adequately manage and ensure the institution's capability against the additional risk. Hence, it is important and necessary to analyze the existence and causes of volatility clustering is the financial time-series.

From Econometrics's perspective, the traditional method to detect the causes of the volatility clustering is the Autoregressive Conditionally Heteroscedastic (ARCH) [3], which is extended to GARCH (Generalized ARCH) [4]. These methods are robust and descriptive approaches to analyze the volatility clustering, but neither of these models explains why such distribution appears. Also, both methods assume a specific distribution for a financial time-series, which even

The associate editor coordinating the review of this manuscript and approving it for publication was Md. Asaduzzaman.

makes the standard estimation process difficult since the long-memory or heavy-tailed characteristics of the financial time-series is changing over time [5]–[7].

From Econophysics' perspective, many researchers have discovered several stylized facts in financial markets. In particular, the heavy tail and aggregated normal distribution of the asset return distribution [8]–[14], asymmetry on rises and falls of the price dynamics, long-range autocorrelation or cross-correlation [7], [15]–[20], volatility clustering [21]–[24] have been studied, which generally suggest the rejection of the traditional normality assumption on the return distribution [25]–[29]. In this context, the volatility clustering has been studied as one of the major stylized facts [5], [23].

At first, the quantitative method can be used to capture the volatility clustering based on the autocorrelations of the return series [2]. Significantly, the evidence of volatility clustering is the positive and slowly decaying (a.k.a. power-law decay) autocorrelation. Note that such power-law decay is observed in the absolute or squared return series, often referred to as the non-linear autocorrelation, rather than the plain log-returns. It is known that the slowly decaying non-linear autocorrelation is mainly due to the correlation between the large fluctuation of volatility clusters. However, it is difficult to assert that the slow decay of nonlinearity implies the long memory tendency of volatility [5]. Nevertheless, if a particular time series has long memory property, or if the distribution of returns is close to non-normality, many statistical estimates tend to possess the autocorrelation or power-law decay [7], [19], [23].

Secondly, there is a network-driven method to detect the volatility clustering based on the fact that the dynamic properties of the time series can be preserved in the network framework. Specifically, many researchers have developed the methods to explain the geometrical structure of the time series, including the cycle approach [30], correlation approach [31], visibility graph [32], recurrence network [33], and isometric network [34]. Also, the monitoring of different patterns of the complex systems in the time-series has been studied [35]–[38]. Among them, we consider the visibility graph to analyze the clustering behavior of the financial time-series based on the following reasons. At first, the visibility graph is known to map the time series into the network values and successfully inherits the time series's properties. In particular, it is known that the visibility graph transforms the random series into a random graph, the periodic series into a regular graph [39], and the fractal series into a scale-free graph [40]–[43]. In this regard, the visibility graph has been utilized in various domains, including the geometric structure of traffic pattern [44], analyzing exchange rate series [45], and reflecting the geometric structure of the two-dimensional Ising algorithm [46]. Secondly, the visibility graph has fast computing time with a simple algorithmic structure, while most complex network-based algorithms require long computing time. Besides, the most recent development of the visibility graph is the Power of Scale-freeness of Visibility Graph (PSVG). Note that this method's feature does not require an infinite time series, so it is easy to implement in the practical usages since the real-world time-series is always finite. Hence, we employ the PSVG for the analyses.

The non-linear autocorrelation and visibility graphs are useful methods to analyze the volatility clustering in the financial time-series. However, there has been a limited attempt to simultaneously incorporate both methods to explain the volatility clustering phenomenon in detail. Therefore, in this study, we suggest the measures for reliable estimation and explanation of the volatility clustering and provide the relevance between two approaches by comparing variations in clustering and fractality measures. In particular, we utilized the clustering and asymmetry measures presented in [22], [24]. Moreover, it is also necessary to measure the degree of influence when the causes of clustering are related. Hence, we analyze the values obtained from the measures of volatility clustering effect. Specifically, we analyze the influence of positive/negative values, large/small fluctuations, and each fluctuation ratio. In addition, the associated asymmetry measures are included to identify the different causes. Note that there are studies on the asymmetry degree, clustering degree, or scale difference according to rising and falling, which are also included in this research [47]–[50].

The rest of this paper is organized as follows. At first, Section 2 presents the methods and measures used in this paper where the Section 2.1, 2.2, and 2.3 explains the clustering index and asymmetric volatility measures, the PSVG approach, and the measures for their variations in different conditions of return distributions, respectively. Then, Section 3 presents the statistical properties and descriptive information of fractality of four representing financial markets, and Section 4 analyzes and discusses the results of the experiments, including the effects on clustering of the distributional features, clustering and asymmetry effects by the scale and sign of the data, and variations effects appear in sequence. Lastly, Section 5 concludes.

II. METHODS

A. CLUSTERING INDEX AND ASYMMETRY

The volatility clustering in the financial time series can be analyzed based on the daily log-return series. Let S_t be the daily closing price of a financial asset at time t, then the daily log-return, R_t, can be defined as

$$R_t = \ln\left(\frac{S_t}{S_{t-1}}\right). \tag{1}$$

The volatility clustering can be quantitatively studied by observing the positive and slowly decaying autocorrelation of the absolute daily log-return series, which indicates the power-law decay behavior. We follow the procedures defined in [22], [24]. Let $C(x_t, x_{t+\tau})$ be the autocorrelation function of time-series variable x for some time interval τ, then

$$C(x, x_{t+\tau}) \equiv \frac{\mathbb{E}\left[(x_t - \mathbb{E}[x_t])(x_{t+\tau} - \mathbb{E}[x_{t+\tau}])\right)}{\sqrt{\mathbb{E}[x_t^2] - (\mathbb{E}[x_t])^2}\sqrt{\mathbb{E}[x_{t+\tau}^2] - \mathbb{E}[x_{t+\tau}]^2}}. \tag{2}$$

Note that the autocorrelation is analyzed to detect the factor contributing to the volatility clustering by comparing the original and Gaussian-rearranged financial return series. The rearrangement procedure can be summarized as follows. At first, we define the Gaussian distribution with its mean and standard deviation analogous to those of the original return series. Secondly, we draw an equal number of data from this Gaussian distribution and refer it as Gaussian simulated series. Thirdly, we sort both the empirical and the simulated series in the descending order according to absolute returns. Lastly, we substitute values in the empirical series by the simulated series one by one from the largest one to the smallest one.

Then, we utilize the clustering index to analyze the volatility clustering in the financial time series. Let c denotes the degree of volatility clustering, indicating the largest $p\%$ within a time window of size n. Given that c is calculated by sliding the moving window with a specified time step, a clustering index, CI_n, for time window n can be defined in terms of the ratio of standard deviation c series such that,

$$CI_n \equiv \frac{\sigma_O}{\sigma_G} \tag{3}$$

where σ_O and σ_G are the standard deviations of the original and Gaussian-rearranged return series for the time window n, respectively. In this regard, CI_n indicates the ratio of clustering patterns within the current data compared to the simulated Gaussian distribution. In case when the clustering is more similar to the original than the simulated Gaussian distribution, the larger the time window size from 1 to 100, the higher the number of largest $p\%$ included in the window. Also, the larger the time window size, the smaller the standard deviation represents the heavier tail. As a result, the larger CI_n is, the higher the degree of volatility clustering is compared to the Gaussian distribution, which indicates the comparatively higher kurtosis and heavier tail. Besides, the theoretical upper limit of the clustering index, $CI_n^{\lim}$, can be derived as described in [22], [24]. Simply put, we can derive a standard deviation of m clustering values using the probability that m corresponding to largest $p\%$ are involved within the window of size n such that,

$$\begin{aligned}\sigma_G &= \sqrt{\sum_{m=0}^{n}\left(m-\frac{p}{100}n\right)^2\left(\frac{p}{100}\right)^m\left(1-\frac{p}{100}\right)^{n-m}} \\ &= \sqrt{n\left(\frac{p}{100}\right)\left(1-\frac{p}{100}\right)}\end{aligned} \tag{4}$$

where $\frac{p}{100}n$ indicates a mean value of c series about window of size n. In this context, the limit of a standard deviation can be defined as follows. For the time series of length N,

$$\begin{aligned}\frac{1}{N-n+1}\Big[&\Big(\frac{p}{100}N-n\Big)\Big(n-\frac{p}{100}n\Big)^2 \\ &+\Big(\Big(1-\frac{p}{100}\Big)N-n\Big)\Big(\frac{p}{100}n\Big)^2 \\ &+\sum_{m=0}^{n}\Big(m-\frac{p}{100}n\Big)^2\Big].\end{aligned} \tag{5}$$

Since $\frac{p}{100}N$ and $\left(1-\frac{p}{100}\right)N$ are larger than n, Eq.(5) converges to $n^2(\frac{p}{100})(1-\frac{p}{100})$. As $N\to\infty$, the theoretical limit of the standard deviation, $\sigma_{\lim}$, converges to

$$\sigma_{\lim} = \sqrt{n^2\left(\frac{p}{100}\right)\left(1-\frac{p}{100}\right)}. \tag{6}$$

Finally, the theoretical upper limit of clustering index, $CI_n^{\lim}$, is,

$$CI_n^{\lim} = \frac{\sigma_{\lim}}{\sigma_G} = \frac{\sqrt{n^2(\frac{p}{100})(1-\frac{p}{100})}}{\sqrt{n(\frac{p}{100})(1-\frac{p}{100})}} = \sqrt{n} \tag{7}$$

In general, the persistence of the volatility can be detected using the GARCH estimation [4], [51], [52], which is widely used to measure the degree of the volatility clustering. However, the GARCH-model only provides the existence of clustering or persistence of the volatility with difficulties in determination of the parameter order, error distribution, the significance of estimated coefficients, and convergence of the algorithm. In contrast, the clustering index does not require such an estimation process. Therefore, the clustering index has its advantage in measuring the degree of volatility clustering in time-series.

Furthermore, the asymmetry of clustering also can be measured. In this study, we employ two asymmetry measures as defined in [22], [24]. The first measure, A_{scale}, evaluates the asymmetry between the largest values and smallest values of the clustering index such that

$$A_{\text{scale}} = \frac{CI^L - CI^S}{CI^L + CI^S} \tag{8}$$

where CI^L and CI^S indicate the clustering indices due to large and small values, respectively. Therefore, the measure shows which of large or small fluctuation contains more clustering as the window size increases. That is, the more large (small) values clustering, the closer A_{scale} is to positive (negative) value. The second measure, A_{sign}, calculates the asymmetry between large positive values and large negative values.

$$A_{\text{sign}} = \frac{CI^+ - CI^-}{CI^+ + CI^-} \tag{9}$$

where CI^+ and CI^- indicate the clustering indices due to large positive returns and large negative returns, respectively. Therefore, we can determine the degree of clustering due to window size and large positive or large negative values. Likewise, positive A_{sign} refers to the existence of more clustering in the positive return series.

B. VISIBILITY GRAPH ALGORITHM

It is possible to map the volatility in times series to its visibility graph [10]. In this graph, the node corresponds to the volatility values, whereas the undirected edge represents the connection between two volatility values when the two nodes satisfy the following condition of the equation.

Let X_i be the i-th point of the time series, then the condition for the existence of the edge is

$$X_{t_c} \leq X_{t_b} + (X_{t_a} - X_{t_b})\frac{X_{t_b} - X_{t_c}}{X_{t_b} - X_{t_a}} \tag{10}$$

where t_a and t_b correspond to the node for specific time(node) in time series, with $t_c(t_a \leq t_c \leq t_b)$. Note that more detailed procedure can be found in [53]. Based on the constructed visibility graph, we count the number of connections in $X_i(i = t_a, \ldots, t_c, \ldots, t_b)$, which can be defined as the k degree of the each node in the undirected graph. In this context, the degree distribution($P(k) = n_k/n$) can b e obtained by calculating the ratio of the total number of nodes(n) to frequency n_k for each k. The degree distribution is known to follow the power-law behaviour, and the power-law exponent(λ) is called as the Power of the Scale freeness in Visibility Graph (PSVG) such that

$$P(k) \sim k^{-\lambda}. \tag{11}$$

The PSVG is closely related to the complexity and fractality in time series. The PSVG has an inverse relationship with the Hurst exponent($H(0 < H < 1)$), which is also related to the autocorrelation in time series. The time-series has the characteristic of the fractional Brownian Motion(fBM) when the λ and H are related as,

$$\lambda = 3 - 2H \tag{12}$$

where $H = 0.5$, $H > 0.5$, and $H < 0.5$ indicate the non-correlated, correlated(persistent), and anti-correlated (anti-persistent) time-series, respectively.

C. MEASURES OF VARIATIONS IN CLUSTERING, ASYMMETRY, AND POWER-LAW EXPONENTS

For instance, if the largest $p\%$ for the measure is set to be 20%, the results of the measures only represent relatively high-risk investments, including extremely large positive and negative returns, which excludes the empirical evidence from the relatively smaller returns. Therefore, we suggest investigating the clustering pattern of volatility in more detail by analyzing the variations within the proposed clustering and asymmetry measures when $p\%$ is changed. In this research, we obtain the variations in measures by comparing the largest 20% and 40%. For the clustering indices (CI^L, CI^S, CI^+, CI^-) and asymmetry measures ($A_{\text{scale}}, A_{\text{sign}}$), the variations can be simply obtained by subtracting the values of 40% from those of 20%.

In addition, we also investigate the variations in PSVG, the power-law coefficients, λ, in visibility graph. If the power-law coefficient is denoted by $\lambda^L(p)$ for largest $p\%$, it can be defined by the coefficient ratio of original data and Gaussian simulated so that the results can be comparable with those of $CI^L, CI^S, CI^+, CI^-, A_{\text{scale}}$ and, A_{sign}. Therefore, the measures regarding the largest $p\%(\lambda^L(p))$, smallest $p\%(\lambda^S(p))$, largest positive $p\%(\lambda^+(p))$, and smallest negative $p\%(\lambda^-(p))$ can be defined such that,

$$\begin{aligned}
\lambda^L(p) &= \frac{\lambda_O^L(p)}{\lambda_G^L(p)} \\
\lambda^S(p) &= \frac{\lambda_O^S(p)}{\lambda_G^S(p)} \\
\lambda^+(p) &= \frac{\lambda_O^+(p)}{\lambda_G^+(p)} \\
\lambda^-(p) &= \frac{\lambda_O^-(p)}{\lambda_G^-(p)}
\end{aligned} \tag{13}$$

where the subscripts O and G on the right-hand side of the equations indicate the original and Gaussian simulated, respectively. Also, the relative difference between largest and smallest value λ_p^{scale}, and that of large positive and large negative value λ_p^{sign} are similarly defined as follows.

$$\begin{aligned}
\lambda^{\text{scale}}(p) &= \lambda^L(p) - \lambda^S(p) \\
\lambda^{\text{sign}}(p) &= \lambda^+(p) - \lambda^-(p)
\end{aligned} \tag{14}$$

Based on the above measures, we can explore the variations in power-law coefficients by subtracting the values of 40% from those of 20%. The methods used in this research are summarized in Figure 1.

III. DATA AND DESCRIPTIVE STATISTICS

In this study, we investigate the four representing financial time-series from different markets including the S&P500(S&PCOMP) for the stock market, one year US Treasury Constant Maturity rate bond(FRTCM1Y) for the bond market, Euro-Dollar exchange rate(EUDOLLR) for the exchange market, and the crude oil price(CRUDOIL) for the commodity markets. Each data obtained from the Thomson Reuters Datastream includes the ten years of daily closing prices from 2009 to 2018, resulting in 2608 observations. For the analysis, we divide the ten years into two sub-periods with equal size. The first sub-period (SP1) is from 2009-01-01 to 2013-12-31, which includes the outbreak of the sub-prime mortgage crisis and the European debt crisis, whereas the second sub-period (SP2) is from 2014-01-01 to 2018-12-31, which does not include any major financial crisis. In this context, the division of sub-period can provide empirical evidence of the volatility clustering in different market conditions. Note that this paper focuses on the impact of the magnitude(large and small values) and the sign(positive and negative values) of volatility on the volatility clustering or fractality by considering the daily return in percent to represent the volatility.

Figure 2 shows the time-varying properties of the financial price and return series. Specifically, the red and yellow lines on the left are the daily returns and absolute return series, respectively, in percent. The black lines on the right are the rearranged Gaussian simulated returns. Note that the vertical dotted lines in each figure represent the division point of the sub-periods. Interestingly, we observe the repeated pattern

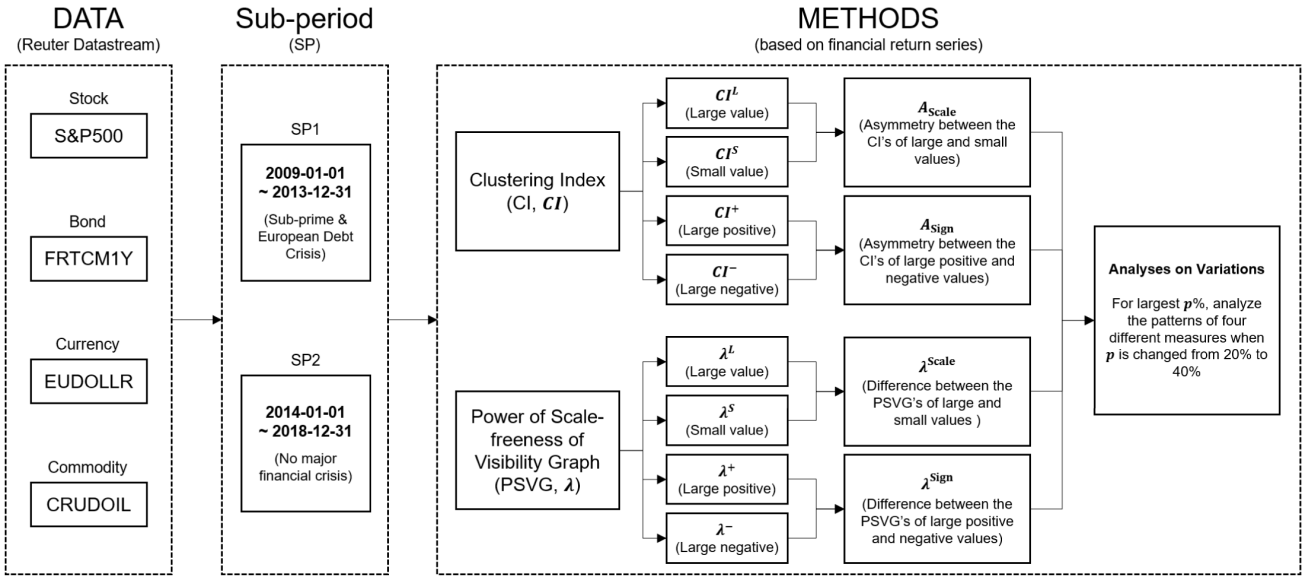

FIGURE 1. Flow chart of the methods used in analyses.

TABLE 1. Descriptive Statistics of return series.

Statistics	S&PCOMP		FRTCM1Y		EUDOLLR		CRUDOIL	
	SP1	SP2	SP1	SP2	SP1	SP2	SP1	SP2
Mean	0.06	0.02	-0.07	0.23	0.00	0.02	0.06	-0.06
Stdev	1.21	0.82	5.94	4.65	0.66	0.52	2.14	2.32
Skewness	-0.26	-0.50	0.18	0.09	-0.25	-0.07	-0.02	0.05
Kurtosis	4.35	4.01	2.52	5.80	2.32	2.23	5.29	2.72
K-S	0.1***	0.15***	0.28***	0.2***	0.12***	0.18***	0.12***	0.15***
Jarque–Bera	1031.35***	917.95***	349.5***	1814.23***	303.65***	268.22***	1504.79***	398.6***
ARCH(10)	207.98***	168.9***	100.74***	116.94***	47.14***	68.57***	258.7***	149.99***
ARCH(20)	298.63***	189.53***	122.72***	154.45***	46.0***	89.92***	300.02***	180.05***
LB(10)	33.83***	16.52*	39.61***	32.74***	5.62	13.44	20.93**	16.14*
LB(20)	50.71***	25.51	69.59***	51.66***	13.42	25.07	35.62**	25.24
$LB(10)^2$	563.04***	354.1***	211.04***	230.31***	64.12***	99.36***	537.29***	318.98***
$LB(20)^2$	948.79***	421.48***	391.29***	415.85***	95.2***	170.32***	963.55***	557.0***
ADF	-16.8***	-17.27***	-8.53***	-8.34***	-36.47***	-36.39***	-18.43***	-39.59***

Note: K-S, LB, and ADF are abbreviations for the Kolmogorov-Smirnov, Ljung-Box, and Augmented Dickey-Fuller tests, respectively.

for large or small absolute returns for all markets and sub-periods, which indicates the volatility clustering property. Specifically, S&PCOMP in Figure 2(a) shows the relatively high volatility in SP1 than that in the SP2. The highest volatility can be found in 2008, which indicates the sub-prime mortgage crisis. Some high volatility points exist in the second sub-period, but it has a much smaller magnitude with shorter duration. In the case of FRTCM1Y in Figure 2(b), constant high volatility is observed from 2008 to 2015, which covers the entire SP1 and the one-third of the SP2. Then, the volatility gradually decreases and becomes extremely small at the end of the SP2. EUDOLLR and CRUDOIL in Figure 2(c,d) show repeated patterns of large and small volatility for both sub-periods. Thus, the various volatility pattern is observed in different financial markets.

The descriptive statistics in Table 1 also shows the different volatility patterns in different financial markets. In the case of S&PCOMP, the mean and standard deviation of the volatility, defined as the daily return series, in SP1 is higher than those of SP2, as suggested in Figure 2(a). The volatility in SP2 was more left-skewed than that of SP1. The volatility in SP1 showed auto-correlation by the Ljung-Box test in lag 10 and 20, whereas the volatility in SP2 shows the weaker auto-correlation. Note that the test statistics on auto-correlation implies that the volatility clustering is higher in SP1 than SP2. In the case of FRTCM1Y, a kurtosis in SP2 is twice larger than that in SP1, whereas the skewness in SP2 is half of that in SP1. In the case of EUDOLLR, unlike other financial assets, the statistics in SP1 and SP2 are analogous in values. In addition, EUDOLLR shows no auto-correlation

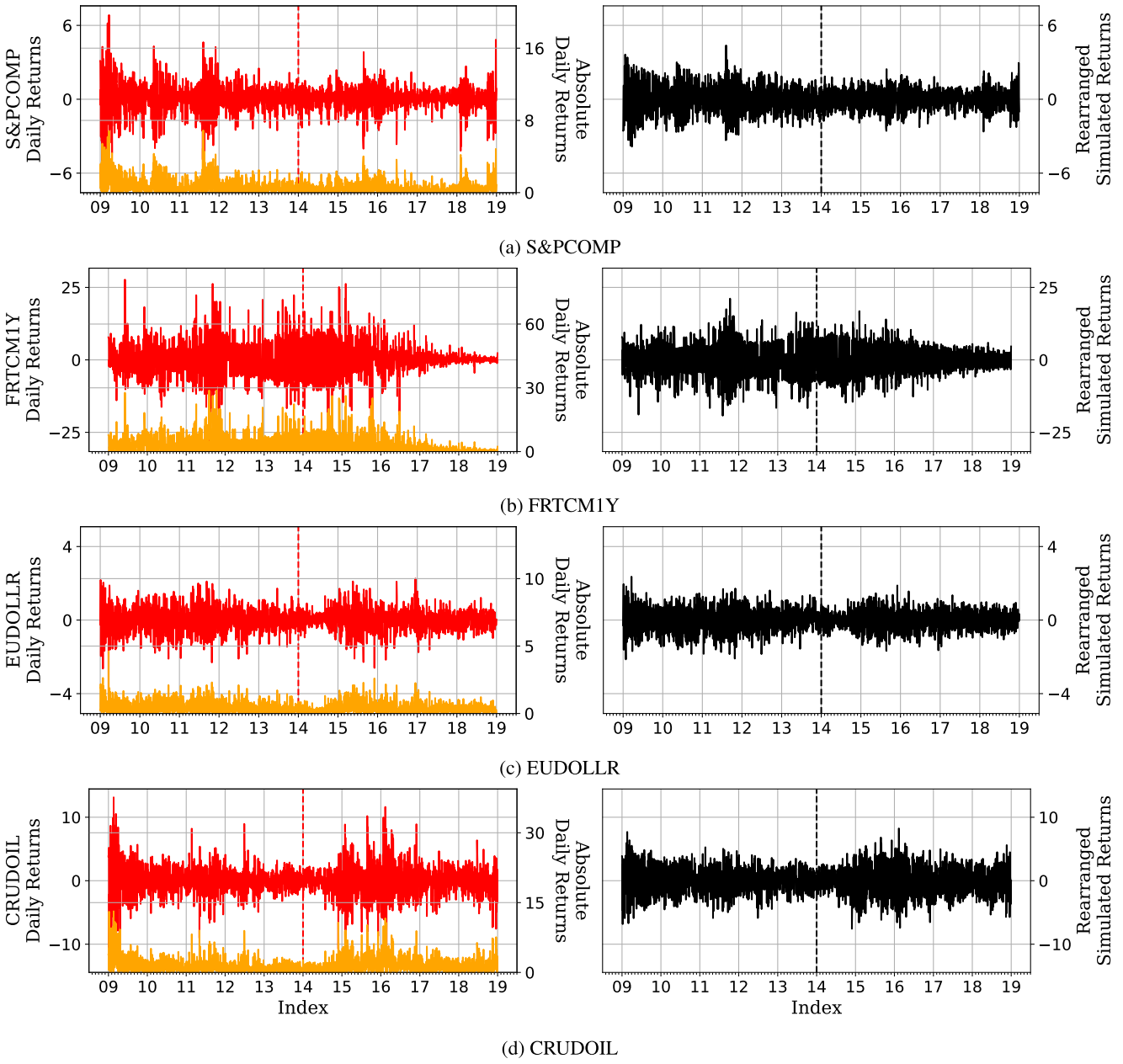

FIGURE 2. **Time series of returns(left) and absolute returns(right) by sub-periods.**

in both sub-period. Lastly, in CRUDOIL, the kurtosis in SP1 is twice greater than that in SP2. Also, the Ljung-Box auto-correlation test indicates weaker auto-correlation in SP2.

Then, we infer the clustering pattern based on the connectedness among distinct volatility values(nodes). At first, Figure 3 illustrates the linear fit to estimate the PSVG on four markets. The horizontal axis is the logarithm of degree k ($1/k$ for minus value), while the vertical axis indicates the logarithm of degree distribution $P(k)$. In addition, blue and red dashed lines result from linear fitting for SP1 and SP2, respectively, with layered areas representing standard error of them. The results show that the degree distribution for each market follows the power-law. The detailed statistics are summarized in Table 2. At first, the PSVGs expressed as a mean$\pm$standard deviation are around 1.6 for all markets and sub-periods. Also, the PSVGs of all markets follow the fractional Brownian motion, whose values can be ranged from 0 to 1. Note that the values of fractional Brownian motion for all markets are ranged between 0.6 and 0.75, implying a persistence behavior. While the descriptive statistics on volatility show significantly different patterns among markets and sub-periods, the descriptive statistics on fractality show similar patterns regardless of market and sub-period.

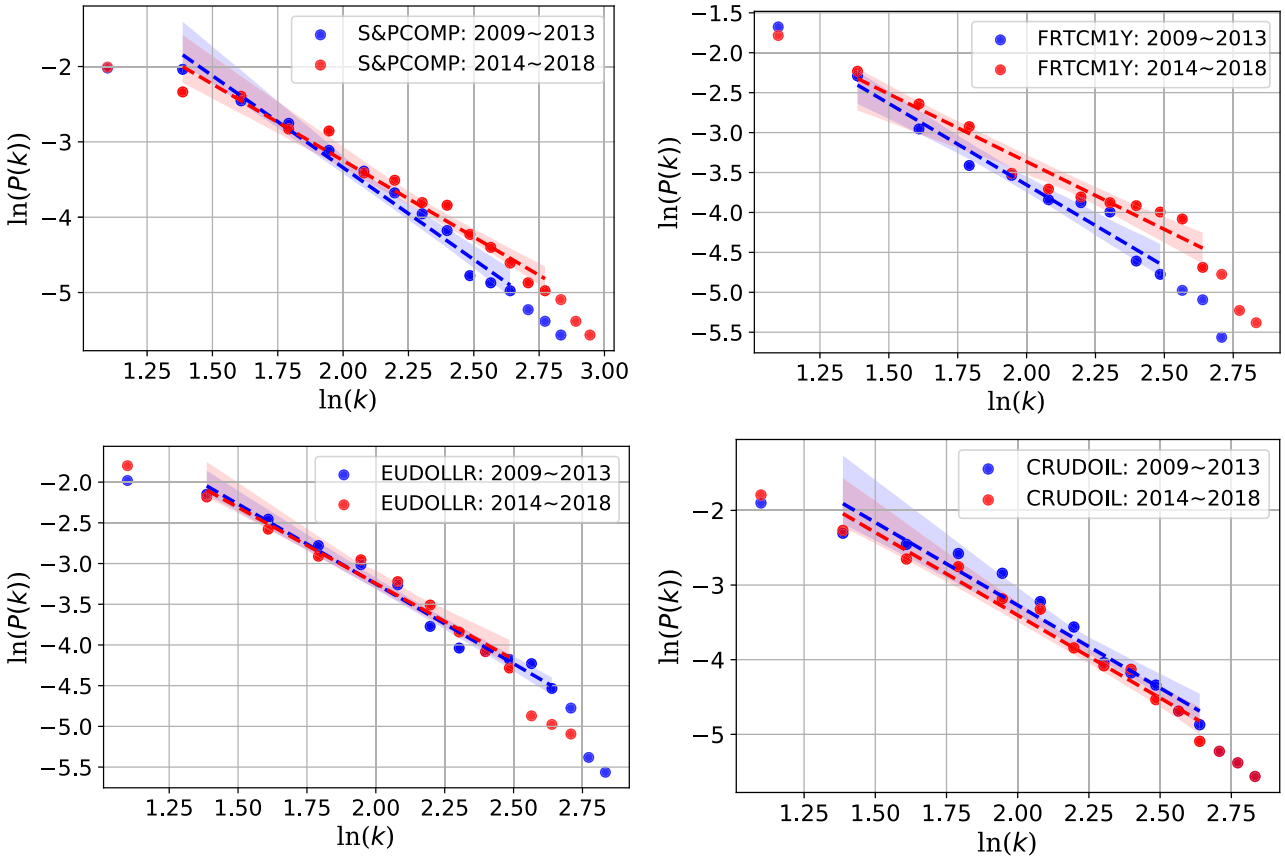

FIGURE 3. The distribution and slope of linear fit (λ_p) for each sub-period.

TABLE 2. Descriptive statistics on fractality.

Market	Sub-periods	power-law	fBM
S&PCOMP	SP1	1.6843±0.1609	0.6579
	SP2	1.5771±0.1362	0.7115
FRTCM1Y	SP1	1.7505±0.1507	0.6247
	SP2	1.5590±0.1418	0.7205
EUDOLLR	SP1	1.6045±0.1607	0.6978
	SP2	1.5913±0.1957	0.7043
CRUDOIL	SP1	1.6593±0.1702	0.6704
	SP2	1.6933±0.1508	0.6534

Note: fBM refers to the fractional Brownian motion.

IV. EMPIRICAL RESULTS AND DISCUSSIONS

A. CLUSTERING DUE TO THE POSITION OF THE DATA IN TIME AND DISTRIBUTIONAL CHARACTERISTICS

Based on the results in Section III, the financial time series shows a high kurtosis or heavy-tail behavior. Thus, it is reasonable to assume that its non-Gaussian distributional property might cause volatility clustering. Figure 4 shows the histograms of the original and Gaussian simulated time-series of four markets. Based on the results, the Gaussian series is simulated correctly, considering the Gaussian fitting on the histogram for all markets and sub-periods. Also, the histogram of the original series is different from the Gaussian simulated series for all markets and sub-periods.

Figure 5 shows the auto-correlation of the absolute return series for the original (red), Gaussian simulated (black), and rearranged Gaussian simulated (blue) data in four markets. For all markets, the original and rearranged Gaussian simulated returns show the positive and slowly decaying behavior, which indicates the existence of volatility clustering. Furthermore, the Gaussian simulated returns' auto-correlation whose values revolve around zero is different from those of the original and rearranged Gaussian simulated returns in all markets and sub-periods. The fact that the auto-correlation of the rearranged Gaussian simulated series is more analogous to that of the original series than that of the Gaussian simulated series implies that the position of the return series's magnitude in time causes the volatility clustering more significantly than its distribution characteristics.

B. VOLATILITY CLUSTERING AND ASYMMETRY DUE TO THE DATA SCALE AND SIGN

We observe that the position of the magnitude of the volatility (absolute return) in time is a significant factor contributing to the volatility clustering. In this regard, we further investigate the factor for different types of returns. At first, we examine

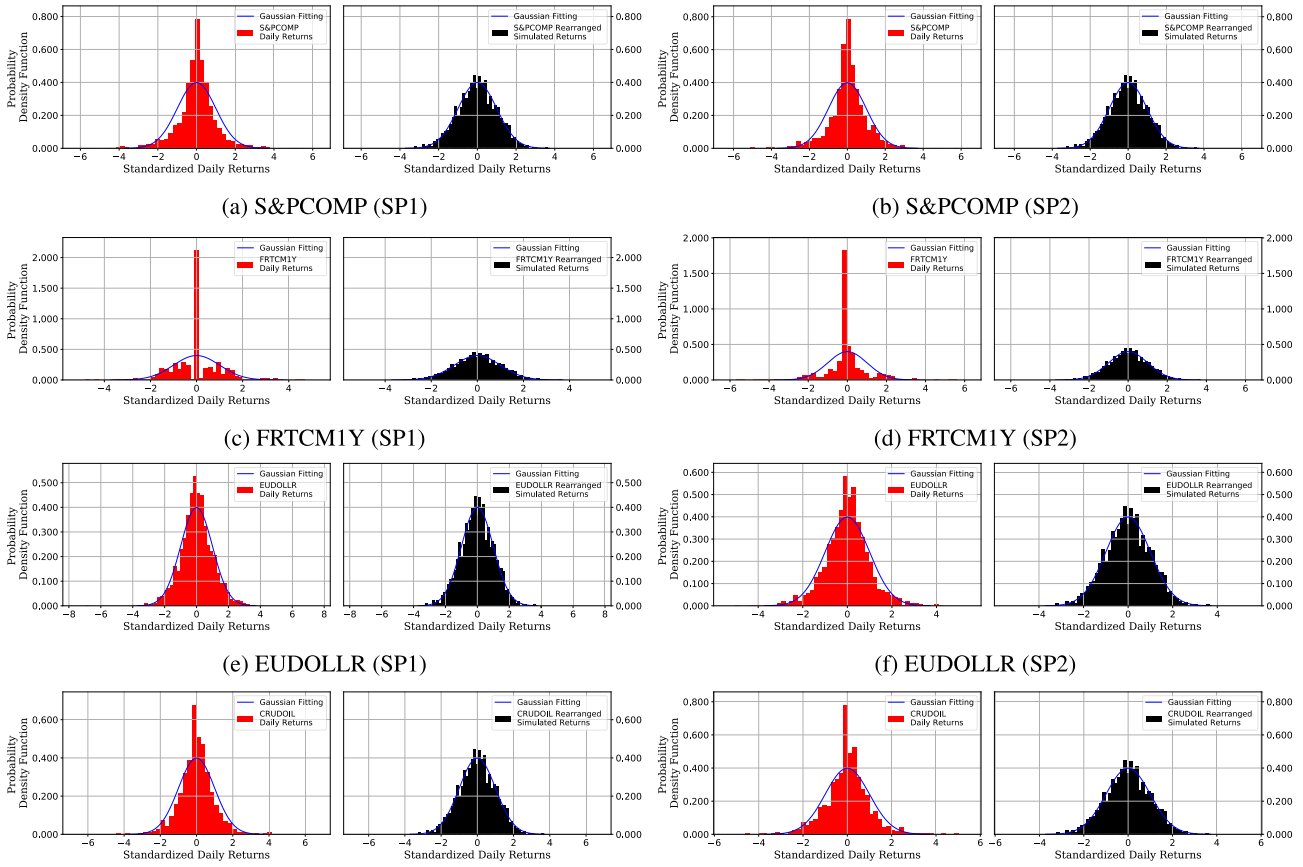

(a) S&PCOMP (SP1) (b) S&PCOMP (SP2)

(c) FRTCM1Y (SP1) (d) FRTCM1Y (SP2)

(e) EUDOLLR (SP1) (f) EUDOLLR (SP2)

(g) CRUDOIL (SP1) (h) CRUDOIL (SP2)

FIGURE 4. **Comparison of histogram plots between the origin time series return(left) and gaussian simulated return(right).**

the clustering effect due to large or small absolute returns. Then, we examine the clustering effect due to the large positive and negative absolute returns. Figure 6 and 7 show the volatility clustering affected by the scale and sign during the SP1 and SP2, respectively, based on the clustering index. Note that the solid black line is the theoretical limit, $CI_n^{\lim}$, and the blue and red lines in the left figures are the CI^L and CI^S, respectively, whereas the blue and red lines in the right figures are the CI^+ and CI^-, respectively. That is, the blue lines indicate how many large returns exist within clustering data(time window) compared to Gaussian distribution, whereas the red lines indicate how many small returns exist within clustering data(time window) compared to Gaussian distribution. Also, the dashed lines indicate the clustering index when $p = 0.2$ (top 20% of the large or small returns), whereas the dash-dotted lines indicate the clustering index when $p = 0.4$ (top 40% of the large or small returns). For all markets and sub-periods, the original data, which exhibits the volatility clustering, possesses more of both large and small returns than the Gaussian distribution. The results imply that large or small returns promote the volatility clustering. Also, there are more of both positive and negative returns in large asset returns ($p = 0.2$). Therefore, the large positive and large negative returns promote the volatility clustering. Note that there are relatively more large returns than small returns in the original data. Besides, the proportion of positive and negative returns in clustering is due to large returns. In summary, the contribution to the clustering effect within top 40% clustering data is Large $>$ Small $>$ Large$(-)$ $>$ Large$(+)$.

The above results separate the contribution of large and small returns(scale) to the clustering effect from that of positive and negative returns(sign) within large returns. Therefore, it is necessary to compare the scale and the sign simultaneously and investigate the difference between sub-periods. In this context, the asymmetry measures are shown in Figure 8. A_{scale}, plotted as the blue line, indicates which of the large returns and small returns has more impact on the clustering, and A_{sign}, plotted as the red line, indicates which of the positive returns and negative returns has more impact on the clustering. During the SP1, the top 20% asset return tends to have many large returns than small returns, with slightly more positive returns than negative returns. In addition, the top 40% volatility also has many large returns with comparatively more negative returns than positive returns. Lastly, as time window size increases, A_{scale} with $p = 0.4$ is

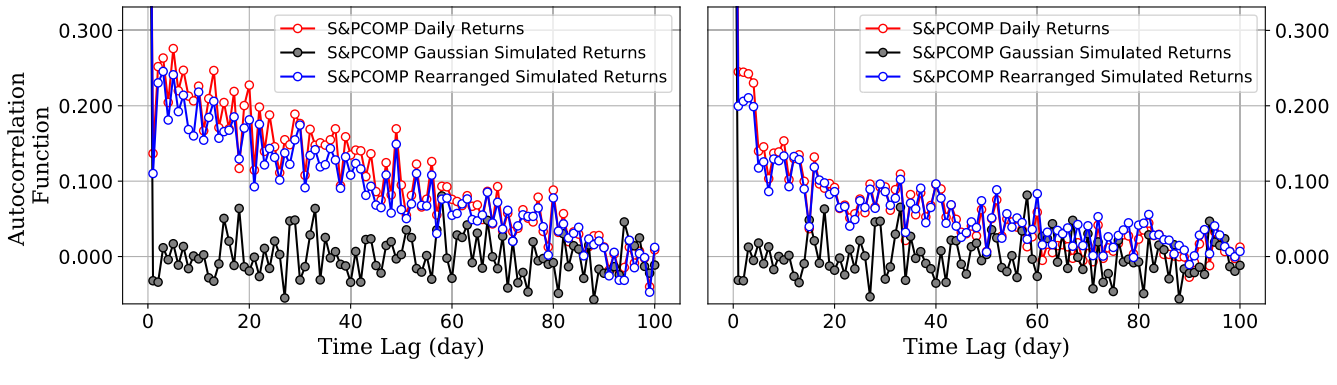

(a) S&PCOMP - SP1(left) and SP2(right)

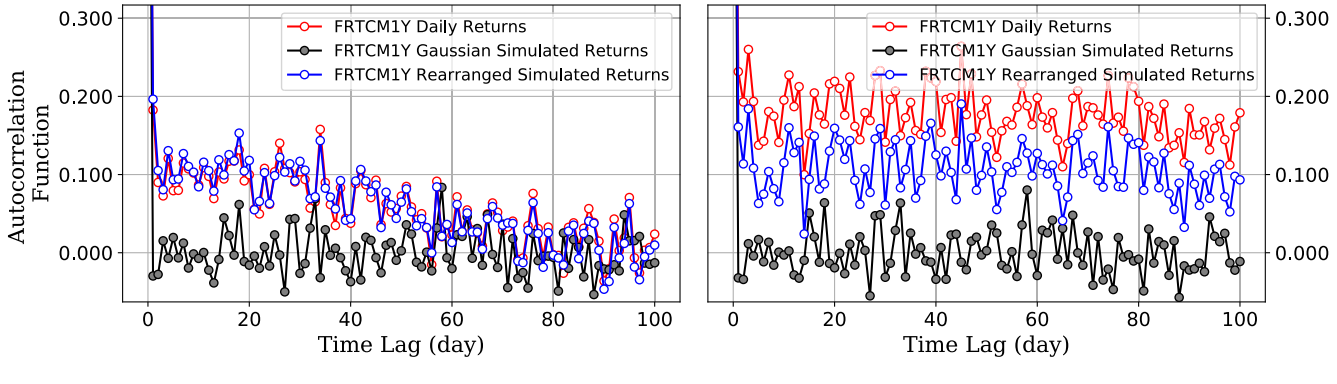

(b) FRTCM1Y - SP1(left) and SP2(right)

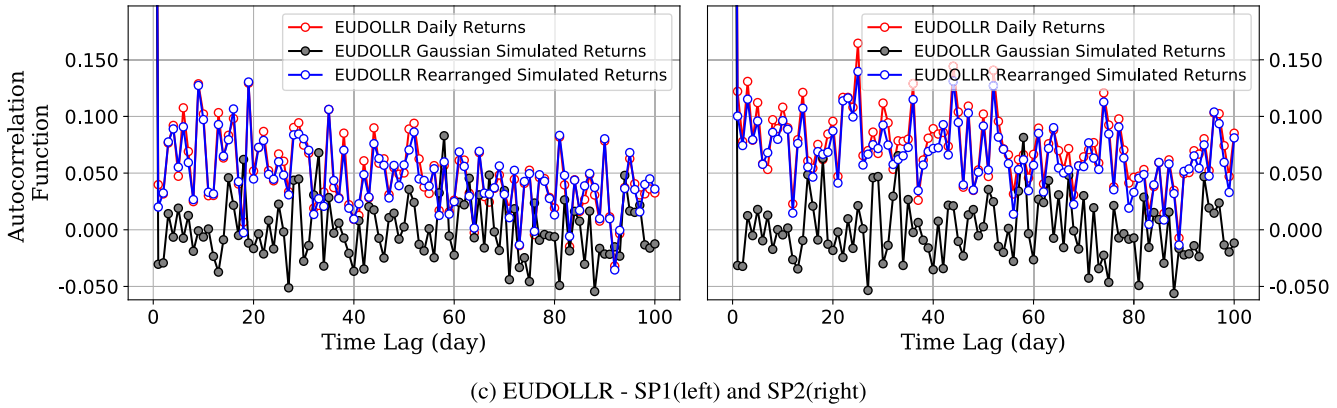

(c) EUDOLLR - SP1(left) and SP2(right)

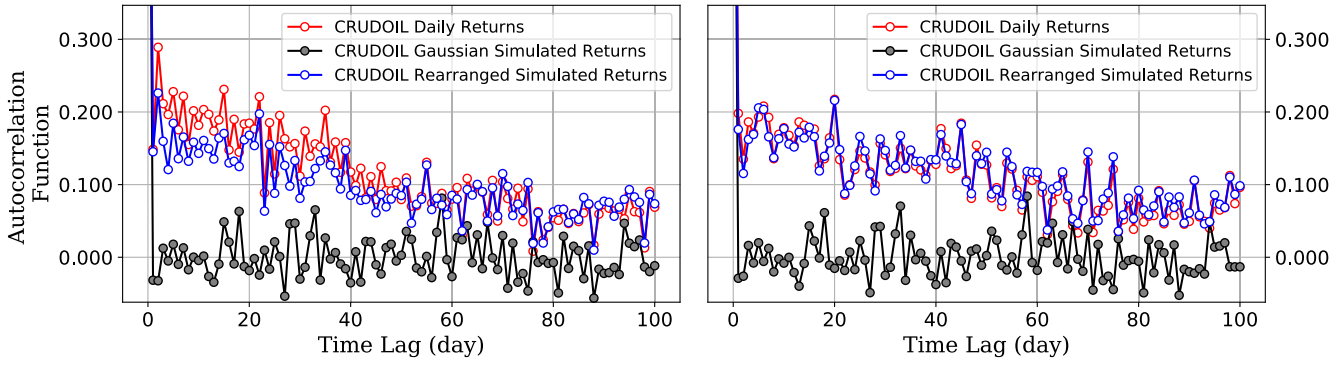

(d) CRUDOIL - SP1(left) and SP2(right)

FIGURE 5. Auto-correlation plots on daily, Gaussian simulated, and rearranged Gaussian simulated returns.

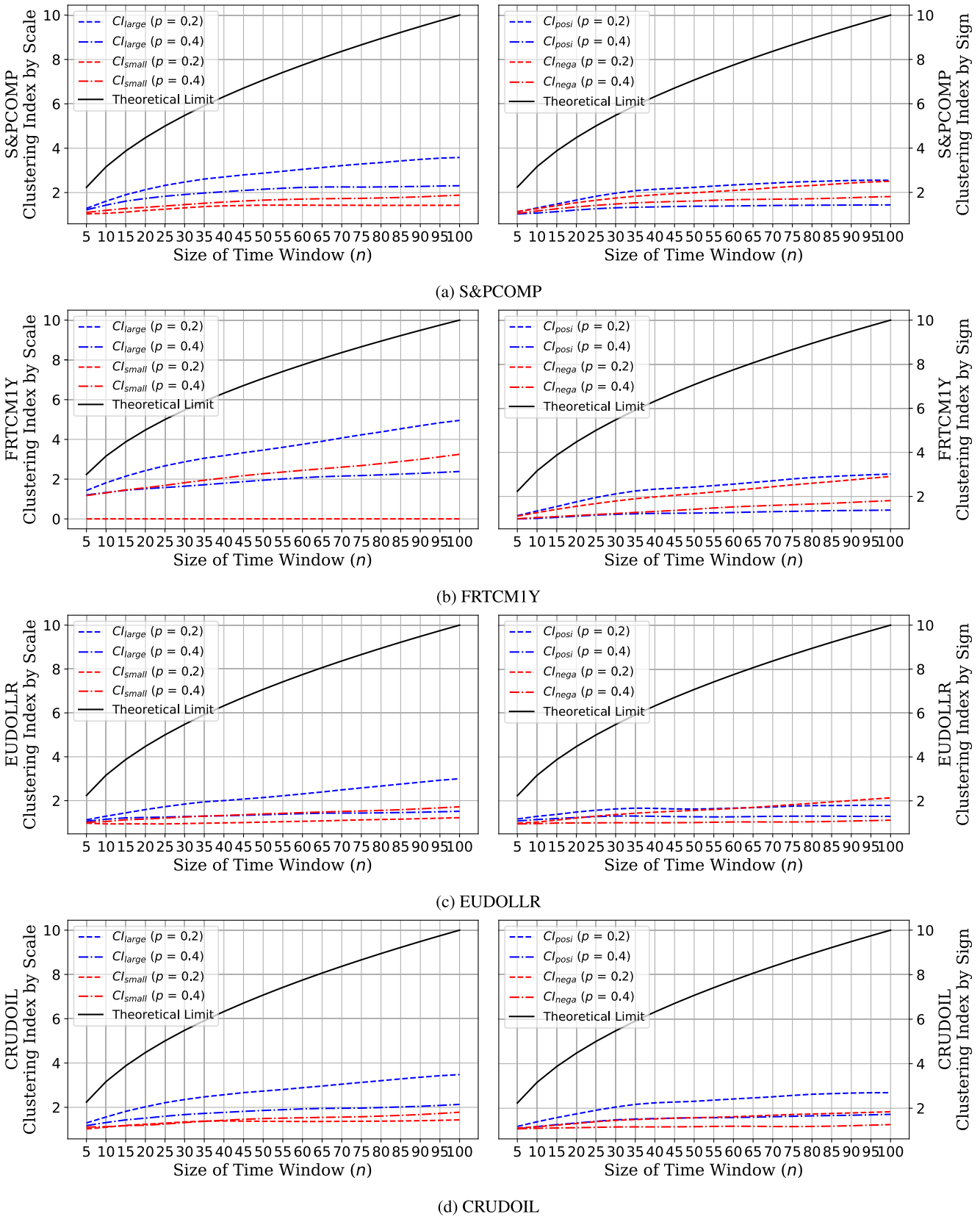

(a) S&PCOMP

(b) FRTCM1Y

(c) EUDOLLR

(d) CRUDOIL

FIGURE 6. Clustering effect by scale(left) and sign(right) during SP1.

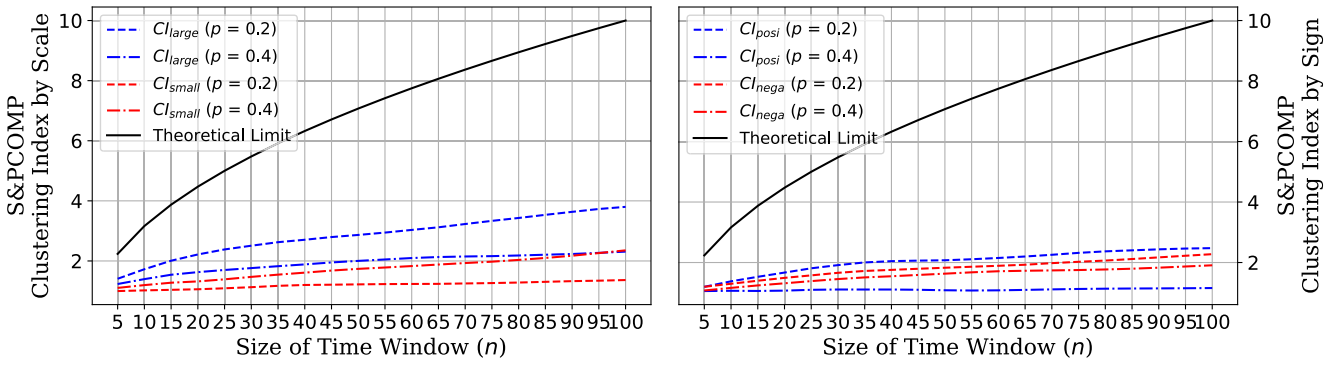

(a) S&PCOMP

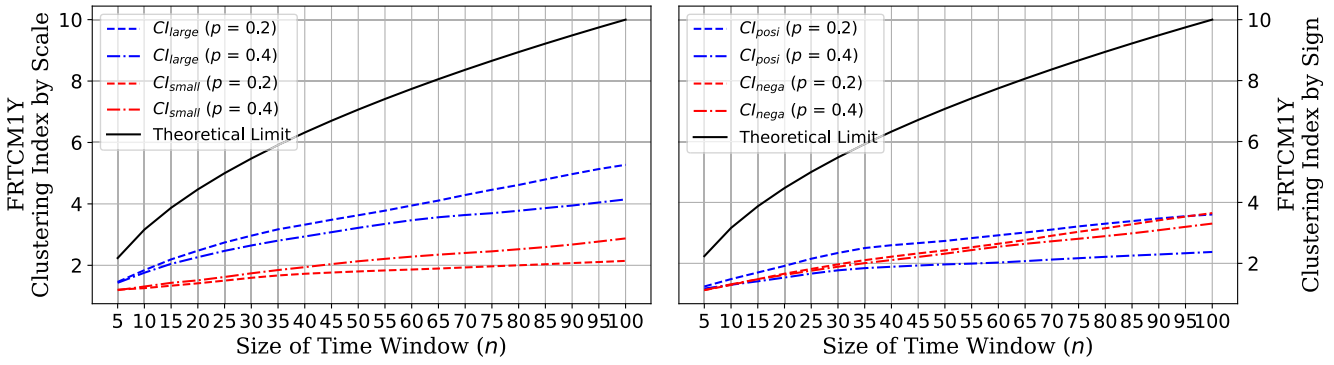

(b) FRTCM1Y

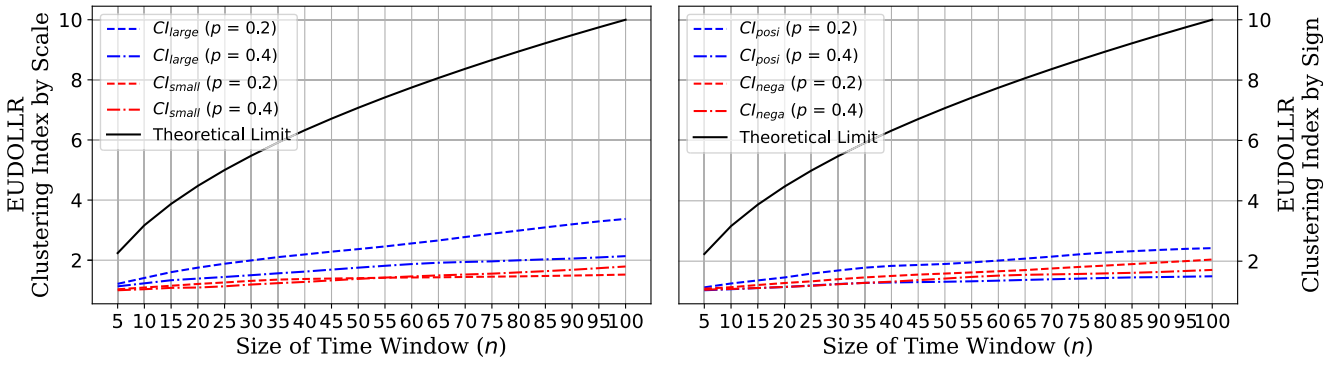

(c) EUDOLLR

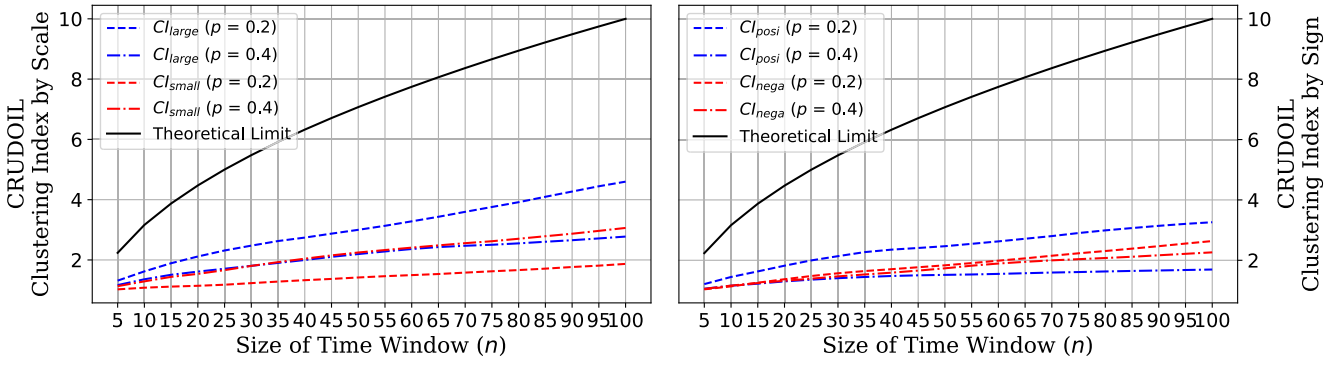

(d) CRUDOIL

FIGURE 7. Clustering effect by scale(left) and sign(right) during SP2.

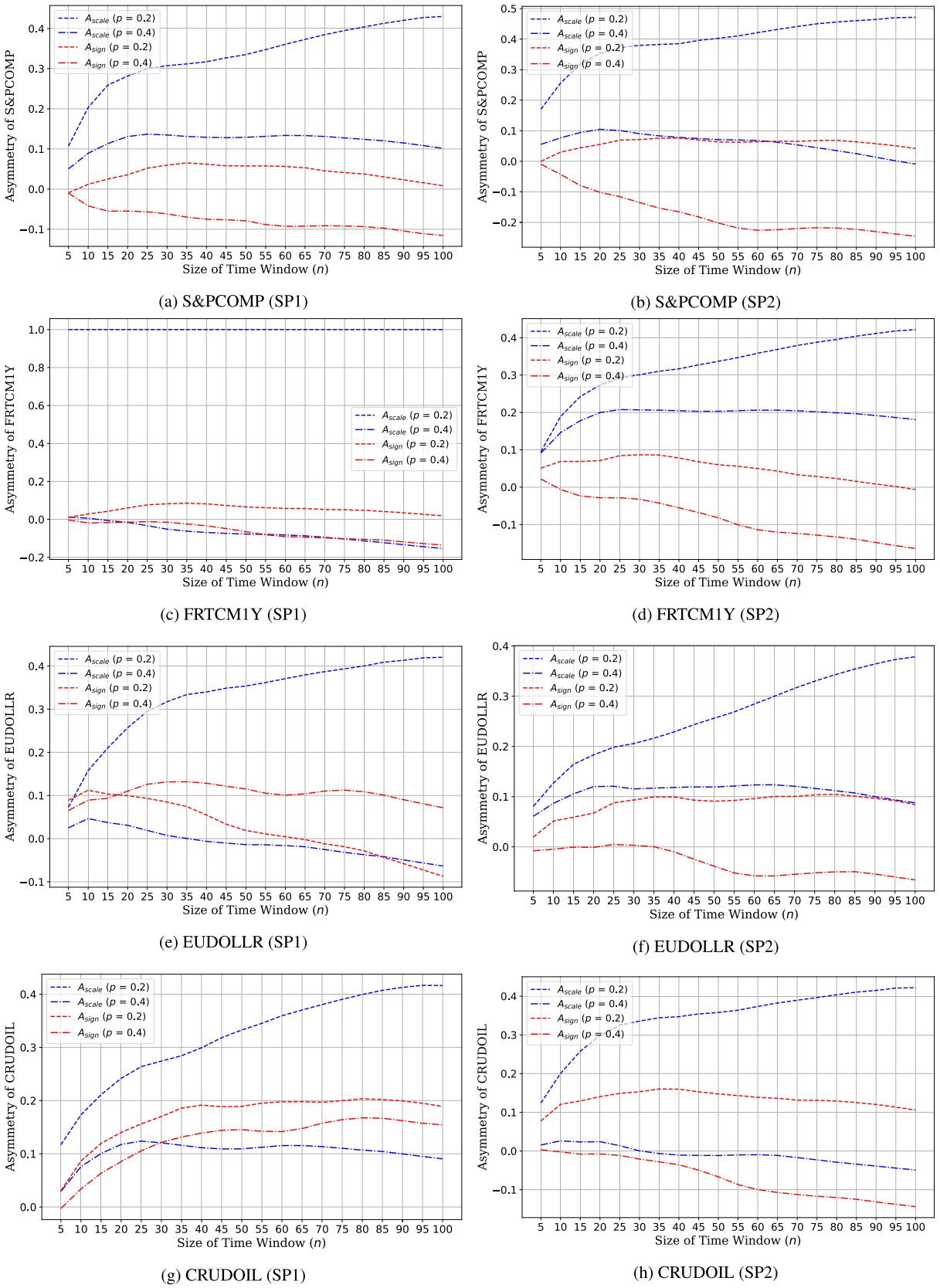

(a) S&PCOMP (SP1)

(b) S&PCOMP (SP2)

(c) FRTCM1Y (SP1)

(d) FRTCM1Y (SP2)

(e) EUDOLLR (SP1)

(f) EUDOLLR (SP2)

(g) CRUDOIL (SP1)

(h) CRUDOIL (SP2)

FIGURE 8. Asymmetry by scale and sign sub-periods.

TABLE 3. Median of clustering index and asymmetry on each market and sub-period.

Markets	Sub-periods	Target Return	Clustering Effect				Asymmetry Effect	
			Large	Large(+)	Large(-)	Small	Scale	Sign
S&PCOMP	SP1	Top 20%	2.92	2.26	2.01	1.42	0.34	0.04
		Top 40%	2.17	1.38	1.63	1.67	0.13	-0.08
	SP2	Top 20%	2.91	2.09	1.84	1.23	0.41	0.06
		Top 40%	2.03	1.1	1.65	1.76	0.07	-0.21
FRTCM1Y	SP1	Top 20%	3.53	2.46	2.16	0	1	0.05
		Top 40%	1.98	1.25	1.45	2.31	-0.08	-0.07
	SP2	Top 20%	3.7	2.78	2.48	1.82	0.34	0.05
		Top 40%	3.28	1.98	2.38	2.17	0.2	-0.09
EUDOLLR	SP1	Top 20%	2.18	1.66	1.59	1.03	0.36	0.01
		Top 40%	1.37	1.29	1.02	1.41	-0.01	0.11
	SP2	Top 20%	2.41	1.93	1.61	1.41	0.26	0.09
		Top 40%	1.78	1.33	1.45	1.4	0.12	-0.04
CRUDOIL	SP1	Top 20%	2.77	2.34	1.58	1.37	0.34	0.19
		Top 40%	1.88	1.57	1.17	1.5	0.11	0.14
	SP2	Top 20%	3.07	2.51	1.87	1.44	0.36	0.13
		Top 40%	2.24	1.52	1.78	2.29	-0.01	-0.08

TABLE 4. Top six ordering patterns of the clustering effects and their ratios and cases of market returns.

Order of Clustering Effect	Ratio	Cases of Market Return
Large > Large(+) > Large(-) > Small	50%	Top 20% All Markets
Large > Large(+) > Small > Large(-)	13%	Top 40% FRTCM1Y(SP2) & CRUDOIL(SP1)
Large > Small > Large(-) > Large(+)	13%	Top 40% S&PCOMP(SP1) & S&PCOMP(SP2)
Small > Large > Large(-) > Large(+)	13%	Top 40% FRTCM1Y(SP1) & CRUDOIL(SP2)
Large > Large(-) > Small > Large(+)	6%	Top 40% EUDOLLR(SP2)
Small > Large > Large(+) > Large(-)	6%	Top 40% EUDOLLR(SP1)

more decreased in SP2 than SP1. However, the overall trend is very similar to that of SP1.

Table 3 summarizes the median of the clustering index and the degree of asymmetry. Note that the median is used to ensure the statistical robustness against dramatic change caused by the time window's small size. In other words, the table shows the degree to which the scale and the sign contribute to the clustering effect of Top 20% and Top 40% returns. In the case of the clustering effect, the clustering effects also become larger when the clustering indices of large, large positive, large negative, and small returns are larger. In the case of the asymmetry effect, the positive(negative) values in the scale column mean small returns have less(more) contribution to clustering in positive(negative) returns. The positive(negative) value in the sign column means positive returns in large return contribute more (less) to clustering than negative return does.

Lastly, the patterns in clustering effect are summarized in Table 4. We reduce the total of sixteen patterns into six major patterns contributing to the volatility clustering. The most frequent pattern, which covers 50%, is the order of Large > Large(+) > Large(−) > Small returns located in the first row. This pattern holds for all markets and sub-periods in the top 20% returns. The larger the asset return and the larger the positive asset return, the higher the volatility clustering and persistent behavior are. In contrast, all the remaining five priority patterns occur in the Top 40% returns. It implies that when lower returns (larger p) is desired, the factors affecting the volatility clustering and persistent behavior can be different according to the market and period. While S&PCOMP consistently shows the order of Large > Small > Large(−) > Large(+) in Top 40% asset return for SP1 and SP2 as described in the third row, EUDOLLR shows different pattern depending on sub-period as listed in the fifth and sixth rows. In the case of FRTCM1Y and CRUDOIL, both the large and small returns can be the most critical factor to the volatility clustering and persistent behavior depending on the sub-periods in the opposite way as described in the second and fourth rows.

C. VARIATIONS OF VOLATILITY CLUSTERING, ASYMMETRY, AND POWER-LAW PROPERTIES

Previously, we discover the factors contributing to the clustering effect according to different markets and the sub-periods. Especially, we observe the establishment of various patterns regarding the order of contributing factors when p is increased from 0.2 to 0.4. Note that the order is the same for all markets and sub-periods when $p = 0.2$. Furthermore, the detailed results on the variations of clustering and asymmetric properties can be investigated in Table 5. Specifically, the pattern of factors contributing to the clustering when extending from high-returns($p = 0.2$) to low-returns($p = 0.4$) are summarized. The variations in six different measures are presented based on the subtraction of the values of $p =$

TABLE 5. Variations of clustering and asymmetry measures from the top 20% to 40% returns on each sub-period.

Variation of Clustering Effect (Top 20% → 40%)							
Sub-period: SP1							
Statistics	**Markets**	**Large**	**Large(+)**	**Large(-)**	**Small**	**Scale**	**Sign**
Values	**S&PCOMP**	-0.75	-0.88	-0.38	0.25	-0.21	-0.12
	FRTCM1Y	-1.55	-1.21	-0.71	2.31	-1.08	-0.12
	EUDOLLR	-0.81	-0.37	-0.57	0.38	-0.37	0.1
	CRUDOIL	-0.89	-0.77	-0.41	0.13	-0.23	-0.05
Directions	**S&PCOMP**	-	-	-	+	-	-
	FRTCM1Y	-	-	-	+	-	-
	EUDOLLR	-	-	-	+	-	+
	CRUDOIL	-	-	-	+	-	-
Sub-period: SP2							
Statistics	**Markets**	**Large**	**Large(+)**	**Large(-)**	**Small**	**Scale**	**Sign**
Values	**S&PCOMP**	-0.88	-0.99	-0.19	0.53	-0.34	-0.27
	FRTCM1Y	-0.42	-0.8	-0.1	0.35	-0.14	-0.14
	EUDOLLR	-0.63	-0.6	-0.16	-0.01	-0.14	-0.13
	CRUDOIL	-0.83	-0.99	-0.09	0.85	-0.37	-0.21
Directions	**S&PCOMP**	-	-	-	+	-	-
	FRTCM1Y	-	-	-	+	-	-
	EUDOLLR	-	-	-	-	-	-
	CRUDOIL	-	-	-	+	-	-

TABLE 6. Variations of power-law properties from the top 20% to 40% returns on each sub-period.

Variation of PSVG (Top 20% → 40%)							
Sub-period: SP1							
Statistics	**Markets**	**Large**	**Large(+)**	**Large(-)**	**Small**	**Scale**	**Sign**
Values	**S&PCOMP**	0.0419	0.0467	0.1409	-0.127	0.695	-0.0580
	FRTCM1Y	0.0540	0.0669	0.4570	-1.2142	2.0159	-0.0812
	EUDOLLR	-0.0378	0.0598	0.1098	-0.0578	0.1383	-0.0499
	CRUDOIL	0.0161	0.0272	0.0412	-0.0468	0.1629	-0.0331
Directions	**S&PCOMP**	+	+	+	-	+	-
	FRTCM1Y	+	+	+	-	+	-
	EUDOLLR	-	+	+	-	+	-
	CRUDOIL	+	+	+	-	+	-
Sub-period: SP2							
Statistics	**Markets**	**Large**	**Large(+)**	**Large(-)**	**Small**	**Scale**	**Sign**
Values	**S&PCOMP**	0.0599	0.2781	0.1624	-0.0550	0.2049	-0.0347
	FRTCM1Y	-0.0095	0.0102	-0.0154	0.0258	-0.0716	0.0822
	EUDOLLR	0.0174	-0.0039	0.0812	-0.0897	0.0364	-0.1208
	CRUDOIL	-0.0189	0.0140	0.0163	-0.0704	0.1603	0.0015
Directions	**S&PCOMP**	+	+	+	-	+	-
	FRTCM1Y	-	+	-	+	-	+
	EUDOLLR	+	-	+	-	+	-
	CRUDOIL	-	+	+	-	+	+

0.4 from those of $p = 0.2$ with its corresponding direction. At first, we examine the results in SP1. For instance, the results of S&PCOMP show that the volatility clustering due to large returns, including the large, large positive, and large negative returns, decreases as p increases (-0.75, -0.88, -0.38). In contrast, the clustering due to small returns increases (0.25). These results are consistent in the other three markets. In terms of asymmetry measures, the volatility clustering is increased by small and large negative returns given that the scale and sign are -0.21 and -0.12, respectively. If each market's result is only considered in terms of the direction, the volatility clustering due to small return increases in all markets. In the case of the direction of asymmetry measures, the clustering due to large negative return becomes larger in all the markets except EUDOLLR when p increases. The result of SP2 is analogous to that of SP1. Both small and large negative return increases in all four markets except EUDOLLR when p increases. That is, EUDOLLR

TABLE 7. Directional consistency between the variations in clustering and asymmetry measures and power-law exponents.

Comparison between clustering and power-law (Top 20% → 40%)								
Sub-period: SP1								
Statistics	**Markets**	**Large**	**Large(+)**	**Large(-)**	**Small**	**Scale**	**Sign**	**#T**
Consistency	**S&PCOMP**	FALSE	FALSE	FALSE	FALSE	FALSE	TRUE	1
	FRTCM1Y	FALSE	FALSE	FALSE	FALSE	FALSE	TRUE	1
	EUDOLLR	TRUE	FALSE	FALSE	FALSE	FALSE	FALSE	1
	CRUDOIL	FALSE	FALSE	FALSE	FALSE	FALSE	TRUE	1
Sub-period: SP2								
Statistics	**Markets**	**Large**	**Large(+)**	**Large(-)**	**Small**	**Scale**	**Sign**	**#T**
Consistency	**S&PCOMP**	FALSE	FALSE	FALSE	FALSE	FALSE	TRUE	1
	FRTCM1Y	TRUE	FALSE	TRUE	TRUE	TRUE	FALSE	4
	EUDOLLR	FALSE	TRUE	FALSE	TRUE	FALSE	TRUE	3
	CRUDOIL	TRUE	FALSE	FALSE	FALSE	FALSE	FALSE	1

Note: #T refers to the number of true among the factor of the volatility clustering in each market.

has more large returns than small returns. Although the market volatility is lower in SP2 than SP1 in four markets, the effect of a factor on the volatility clustering remains the same even under the non-Gaussian distribution. In summary, the volatility clustering of the low-returns($p = 0.4$) is more affected by the small return and large negative returns than the high-returns($p = 0.2$).

Furthermore, we summarize the variation of fractality in Eqs.(13) and (14) in Table 6. Similar to the Table 5, we describe how PSVG changes when p increases from 0.2 (high-return) to 0.4 (low-return). Note that the positive value and direction indicate the increases in persistent behavior in volatility clustering, whereas the negative value and direction indicate the increases in anti-persistent behavior. For instance, the result of S&PCOMP in SP1 shows that the large returns (0.0299, 0.0655, 0.1314) increase the persistent behavior in volatility clustering, whereas the small returns contribute to the increase in anti-persistent behavior. The same results can be found on the scale. Also, anti-persistent behavior is more increased by large negative values than large positive values. That is, small and large negative returns, critical factors in the clustering effect, increase the anti-persistent behavior of volatility clustering. Again, all the four markets except EUDOLLR shows the same pattern. Unlike SP1, the variations in PSVG in SP2 are hardly generalized for different markets. While S&PCOMP in SP2 has the same pattern in SP1, all the other markets have distinct fractality patterns. In other words, unlike clustering and asymmetry measures, the PSVG are highly affected by non-Gaussian distribution. Note that the return distribution of SP2 is closer to the Gaussian distribution than that of SP1 for all markets. It implies that the clustering and asymmetry measures are more robust than the PSVG in terms of generalization of the pattern of factors contributing to the volatility clustering.

Lastly, Table 7 summarizes the comparison whether the sign of directions in Table 5 and that of in Table 6 are the same. Given that the number of trues in SP1 is much smaller than that in SP2, we presume that the directions of clustering and asymmetry measures when p increases from 0.2 to 0.4 and that of PSVG changes in opposite direction when the market is highly volatile.

V. CONCLUSION

The prices of numerous financial products in the market change over time and generate various financial time-series patterns. In particular, volatility clustering exists, indicating the phenomenon that the large (small) fluctuations of the financial time-series consistently occur after the previous large (small) fluctuations. There have been efforts to detect the volatility clustering and explain the causes of the volatility clustering within the market. In this study, we accumulate state-of-the-art methods and analyzed volatility clustering using the non-linear autocorrelation and various clustering and asymmetry measures. We also provide a further explanation of the causes of the volatility clustering when the target return is changed. Note that, to the best of our knowledge, this is the first attempt to utilize clustering and asymmetry measures to analyze the volatility clustering simultaneously, including their variations with respect to the target returns.

The findings of this paper are as follows. In terms of the existence of volatility clustering, we observe that volatility clustering occurs in all representative financial time series of the four financial markets where the return distributions follow the fractional Brownian motion rather than the Gaussian distribution in most markets and sub-periods. Also, we confirm that the data positioning of the return series contributes more to the volatility clustering than the distributional characteristics such as heavy-tails. Specifically, we observe that the four representative financial return-series show the positive and slowly decaying non-linear autocorrelation. Also, we confirm that the Gaussian simulated returns, whose order of returns are rearranged as the underlying real financial time-series, also show the power-law decay.

The results above are further investigated by the clustering and asymmetry measures. In particular, the factors affecting the volatility clustering are studied in detail. At first,

we observe that the order of contributing factors on volatility clustering is Large > Large positive > Large negative > Small returns for high target return (small p). In contrast, the order of contributions of the factors appears differently depending on the market conditions. Secondly, in most markets and sub-periods, we discover that the scale of the return contributes more to volatility clustering than its sign. It implies that the extreme upward or downward price movement might last longer when realized. Thirdly, we find that irrespective of market conditions, the group who obtain high returns tends to keep their high returns where the order of contributing factors are independent of the market or sub-periods since the clustering and asymmetry measures show the similar pattern regardless of market condition. In contrast, the variation of PSVG shows different contributing factors depending on market conditions. During the financial crisis (SP1), the direction of increase or decrease in PSVG is similar for all contributing factors. However, after the financial crisis (SP2), the direction of increase or decrease in PSVG varies depending on the market and contributing factors. Given that the financial crisis and non-financial crisis periods show different return distributions, the PSVG coefficients seem to be affected by the non-Gaussian distribution, unlike clustering and asymmetry measures. Therefore, we presume that clustering and asymmetry measures are more robust measures to distribution for the volatility clustering than PSVG. Lastly, in a highly volatile market, an inverse relationship between the directions of the clustering effect defined by the clustering indices and asymmetry and PSVG is observed when the variation is examined from high returns to low returns.

Based on the empirical evidences, we conclude that the volatility clustering in the financial time-series exists whose contributing factors varies for market condition and target returns. Therefore, as a future work, we are planning to model the Value-at-Risk and Expected Shortfall algorithms, switching with respect to volatility clustering incurred from different causes. Such algorithms can be further implemented in terms of decentralized in financial risk management system.

REFERENCES

[1] L. Bachelier, "Théorie de la spéculation," in *Annales scientifiques de l'École normale supérieure*, vol. 17. 1900, pp. 21–86.
[2] Z. Ding, C. W. J. Granger, and R. F. Engle, "A long memory property of stock market returns and a new model," *J. Empirical Finance*, vol. 1, no. 1, pp. 83–106, Jun. 1993.
[3] R. F. Engle, "Autoregressive conditional heteroscedasticity with estimates of the variance of United Kingdom inflation," *Econometrica, J. Econ. Soc.*, vol. 50, no. 4, pp. 987–1007, 1982.
[4] T. Bollerslev, "Generalized autoregressive conditional heteroskedasticity," *J. Econometrics*, vol. 31, no. 3, pp. 307–327, Apr. 1986.
[5] R. Cont, "Volatility clustering in financial markets: Empirical facts and agent-based models," in *Long Memory in Economics*. Berlin, Germany: Springer, 2007, pp. 289–309.
[6] S. I. Resnick, "Why non-linearities can ruin the heavy-tailed modeler's day," in *A Practical Guide to Heavy Tails: Statistical Techniques and Applications*. Boston, MA, USA: Birkhäuser, 1998, pp. 219–239.
[7] S. Resnick, G. Samorodnitsky, and F. Xue, "How misleading can sample ACFs of stable MAs be? (very!)," *Ann. Appl. Probab.*, vol. 9, no. 3, pp. 797–817, Aug. 1999.
[8] R. N. Mantegna and H. E. Stanley, "Scaling behaviour in the dynamics of an economic index," *Nature*, vol. 376, no. 6535, p. 46, 1995.
[9] B.-H. Wang and P.-M. Hui, "The distribution and scaling of fluctuations for Hang Seng index in Hong Kong stock market," *Eur. Phys. J. B-Condens. Matter Complex Syst.*, vol. 20, no. 4, pp. 573–579, 2001.
[10] A. Razdan, "Scaling in the Bombay stock exchange index," *Pramana*, vol. 58, no. 3, pp. 537–544, Mar. 2002.
[11] J. A. Skjeltorp, "Scaling in the Norwegian stock market," *Phys. A, Stat. Mech. Appl.*, vol. 283, nos. 3–4, pp. 486–528, Aug. 2000.
[12] P. Gopikrishnan, V. Plerou, Y. Liu, L. N. Amaral, X. Gabaix, and H. E. Stanley, "Scaling and correlation in financial time series," *Phys. A, Stat. Mech. Appl.*, vol. 287, nos. 3–4, pp. 362–373, 2000.
[13] H. E. Stanley, L. A. N. Amaral, P. Gopikrishnan, and V. Plerou, "Scale invariance and universality of economic fluctuations," *Phys. A, Stat. Mech. Appl.*, vol. 283, nos. 1–2, pp. 31–41, Aug. 2000.
[14] P. Gopikrishnan, M. Meyer, L. A. N. Amaral, and H. E. Stanley, "Inverse cubic law for the distribution of stock price variations," *Eur. Phys. J. B*, vol. 3, no. 2, pp. 139–140, Jul. 1998.
[15] F. Lillo and J. D. Farmer, "The long memory of the efficient market," *Stud. Nonlinear Dyn. Econometrics*, vol. 8, no. 3, pp. 1–19, Jan. 2004.
[16] J. Jiang, K. Ma, and X. Cai, "Non-linear characteristics and long-range correlations in Asian stock markets," *Phys. A, Stat. Mech. Appl.*, vol. 378, no. 2, pp. 399–407, May 2007.
[17] B. Mandelbrot, "New methods in statistical economics," *J. Political Economy*, vol. 71, no. 5, pp. 421–440, Oct. 1963.
[18] B. B. Mandelbrot, "The variation of certain speculative prices," in *Fractals and Scaling in Finance*. New York, NY, USA: Springer, 1997, pp. 371–418.
[19] R. Adler, R. Feldman, and M. Taqqu, *A Practical Guide to Heavy Tails: Statistical Techniques and Applications*. Boston, MA, USA: Birkhäuser, 1998.
[20] B. Podobnik, D. Horvatic, A. M. Petersen, and H. E. Stanley, "Cross-correlations between vol. change, and price change," *Proc. Nat. Acad. Sci. USA*, vol. 106, no. 52, pp. 22079–22084, 2009.
[21] J. Y. Campbell, A. W. Lo, A. C. MacKinlay, and R. F. Whitelaw, "The econometrics of financial markets," *Macroeconomic Dyn.*, vol. 2, no. 4, pp. 559–562, 1998.
[22] J.-J. Tseng and S.-P. Li, "Asset returns and volatility clustering in financial time series," *Phys. A, Stat. Mech. Appl.*, vol. 390, no. 7, pp. 1300–1314, Apr. 2011.
[23] G. Teyssière and A. P. Kirman, *Long Memory in Economics*. Berlin, Germany: Springer, 2006.
[24] J.-J. Tseng and S.-P. Li, "Quantifying volatility clustering in financial time series," *Int. Rev. Financial Anal.*, vol. 23, pp. 11–19, Jun. 2012.
[25] R. Cont, "Empirical properties of asset returns: Stylized facts and statistical issues," *Quant. Finance*, vol. 1, no. 2, pp. 223–236, Feb. 2001.
[26] R. F. Engle and A. J. Patton, "What good is a volatility model?" in *Forecasting Volatility in the Financial Markets*. Amsterdam, The Netherlands: Elsevier, 2007, pp. 47–63.
[27] A. Chakraborti, I. M. Toke, M. Patriarca, and F. Abergel, "Econophysics: Empirical facts and agent-based models," 2009, *arXiv:0909.1974*. [Online]. Available: http://arxiv.org/abs/0909.1974
[28] R. N. Mantegna and H. E. Stanley, *Introduction to Econophysics: Correlations and Complexity in Finance*. Cambridge, U.K.: Cambridge Univ. Press, 1999.
[29] J.-P. Bouchaud and M. Potters, *Theory of Financial Risk and Derivative Pricing: From Statistical Physics to Risk Management*. Cambridge, U.K.: Cambridge Univ. Press, 2003.
[30] J. Zhang and M. Small, "Complex network from pseudoperiodic time series: Topology versus dynamics," *Phys. Rev. Lett.*, vol. 96, no. 23, Jun. 2006, Art. no. 238701.
[31] Y. Yang and H. Yang, "Complex network-based time series analysis," *Phys. A, Stat. Mech. Appl.*, vol. 387, nos. 5–6, pp. 1381–1386, 2008.
[32] L. Lacasa, B. Luque, F. Ballesteros, J. Luque, and J. C. Nuño, "From time series to complex networks: The visibility graph," *Proc. Nat. Acad. Sci. USA*, vol. 105, no. 13, pp. 4972–4975, Apr. 2008.
[33] X. Xu, J. Zhang, and M. Small, "Superfamily phenomena and motifs of networks induced from time series," *Proc. Nat. Acad. Sci. USA*, vol. 105, no. 50, pp. 19601–19605, 2008.
[34] Y. Zhao, T. Weng, and S. Ye, "Geometrical invariability of transformation between a time series and a complex network," *Phys. Rev. E, Stat. Phys. Plasmas Fluids Relat. Interdiscip. Top.*, vol. 90, no. 1, Jul. 2014, Art. no. 012804.

[35] S. Mutua, C. Gu, and H. Yang, "Visibility graphlet approach to chaotic time series," *Chaos, Interdiscipl. J. Nonlinear Sci.*, vol. 26, no. 5, May 2016, Art. no. 053107.
[36] M. Stephen, C. Gu, and H. Yang, "Visibility graph based time series analysis," *PLoS ONE*, vol. 10, no. 11, Nov. 2015, Art. no. e0143015.
[37] M. McCullough, M. Small, T. Stemler, and H. H.-C. Iu, "Time lagged ordinal partition networks for capturing dynamics of continuous dynamical systems," *Chaos, Interdiscipl. J. Nonlinear Sci.*, vol. 25, no. 5, May 2015, Art. no. 053101.
[38] J. Zhang, J. Zhou, M. Tang, H. Guo, M. Small, and Y. Zou, "Constructing ordinal partition transition networks from multivariate time series," *Sci. Rep.*, vol. 7, no. 1, pp. 1–13, Dec. 2017.
[39] M. E. J. Newman, D. J. Watts, and S. H. Strogatz, "Random graph models of social networks," *Proc. Nat. Acad. Sci. USA*, vol. 99, no. 1, pp. 2566–2572, 2002.
[40] A.-L. Barabási and R. Albert, "Emergence of scaling in random networks," *Science*, vol. 286, no. 5439, pp. 509–512, Oct. 1999.
[41] R. Albert and A.-L. Barabási, "Statistical mechanics of complex networks," *Rev. Mod. Phys.*, vol. 74, p. 47, Jan. 2002.
[42] L. Lacasa, B. Luque, J. Luque, and J. C. Nuño, "The visibility graph: A new method for estimating the Hurst exponent of fractional Brownian motion," *Europhys. Lett.*, vol. 86, no. 3, p. 30001, 2009.
[43] M. Ahmadlou, H. Adeli, and A. Adeli, "Improved visibility graph fractality with application for the diagnosis of autism spectrum disorder," *Phys. A, Stat. Mech. Appl.*, vol. 391, no. 20, pp. 4720–4726, Oct. 2012.
[44] M. Andjelković, N. Gupte, and B. Tadić, "Hidden geometry of traffic jamming," *Phys. Rev. E, Stat. Phys. Plasmas Fluids Relat. Interdiscip. Top.*, vol. 91, no. 5, May 2015, Art. no. 052817.
[45] Y. Yang, J. Wang, H. Yang, and J. Mang, "Visibility graph approach to exchange rate series," *Phys. A, Stat. Mech. Appl.*, vol. 388, no. 20, pp. 4431–4437, Oct. 2009.
[46] L. Zhao, W. Li, C. Yang, J. Han, Z. Su, and Y. Zou, "Multifractality and network analysis of phase transition," *PLoS ONE*, vol. 12, no. 1, Jan. 2017, Art. no. e0170467.
[47] O. Henry, "Modelling the asymmetry of stock market volatility," *Appl. Financial Econ.*, vol. 8, no. 2, pp. 145–153, Apr. 1998.
[48] A. Peiró, "Asymmetries and tails in stock index returns: Are their distributions really asymmetric?" *Quant. Finance*, vol. 4, no. 1, pp. 37–44, Feb. 2004.
[49] J. Chen, H. Hong, and J. C. Stein, "Forecasting crashes: Trading volume, past returns, and conditional skewness in stock prices," *J. Financial Econ.*, vol. 61, no. 3, pp. 345–381, 2001.
[50] M. M. Pelagatti, "Modelling good and bad volatility," *Stud. Nonlinear Dyn. Econometrics*, vol. 13, no. 1, pp. 1–13, Jan. 2009.
[51] D. B. Nelson, "Conditional heteroskedasticity in asset returns: A new approach," *Econometrica, J. Econ. Soc.*, vol. 59, no. 2, pp. 347–370, 1991.
[52] R. T. Baillie, T. Bollerslev, and H. O. Mikkelsen, "Fractionally integrated generalized autoregressive conditional heteroskedasticity," *J. Econometrics*, vol. 74, no. 1, pp. 3–30, Sep. 1996.
[53] M. Mondal, A. Mondal, J. Mondal, K. K. Patra, A. Deb, and D. Ghosh, "Evidence of centrality dependent fractal behavior in high energy heavy ion interactions: Hint of two different sources," *Chaos, Solitons Fractals*, vol. 113, pp. 230–237, Aug. 2018.

KYUNGWON KIM received the B.Sc. degree in mathematics and physics from Hanyang University, Seoul, South Korea, in 2007, and the M.Sc. degree in computational science and technology (specialized in data mining) and the Ph.D. degree in industrial engineering (specialized in financial engineering) from Seoul National University, Seoul, in 2010 and 2014, respectively. From 2014 to mid-2017, he was a Data Scientist with the Big Data Laboratory, Visual Display Division, Samsung Electronics Company Ltd., South Korea. Then, he moved to the AI Center of Samsung Research and currently working as a Senior Data Scientist, focusing on sales and marketing analytics based on data mining, time-series, and explainable AI.

JAE WOOK SONG received the B.Sc. degree in industrial engineering from the Georgia Institute of Technology, in 2010, and the Ph.D. degree in industrial engineering from Seoul National University, in 2016. Then, he had been working as a Senior Data Scientist with Samsung Electronics Company Ltd., and an Assistant Professor of data science with Sejong University. In 2019, he joined the Department of Industrial Engineering, Hanyang University, where he is currently an Assistant Professor running the Financial Innovation and Analytics Laboratory. His research interests include inter- and multi-disciplinary approaches for data-driven innovations in financial markets, risk management, investment strategies, portfolio management, and business analytics.